Journal of Computational and Applied Mathematics 287 (2015) 98–114

Contents lists available at ScienceDirect

Journal of Computational and Applied Mathematics

journal homepage: www.elsevier.com/locate/cam

Phase portraits of uniform isochronous quartic centers

Jackson Itikawa, Jaume Llibre *

Departament de Matemàtiques, Universitat Autònoma de Barcelona, 08193 Bellaterra, Barcelona, Catalonia, Spain

ARTICLE INFO

Article history:
Received 16 September 2014
Received in revised form 21 January 2015

MSC:
primary 34C05
34C25

Keywords:
Polynomial vector field
Uniform isochronous center
Phase portrait

ABSTRACT

In this paper we classify the global phase portraits in the Poincaré disc of all quartic polynomial differential systems with a uniform isochronous center at the origin such that their nonlinear part is not homogeneous.

1. Introduction and statement of the main results

Christian Huygens is credited with being one of the first scholars to study isochronous systems in the XVII century, even before the development of the differential calculus. Huygens investigated the cycloidal pendulum, which has isochronous oscillations in opposition to the monotonicity of the period of the usual pendulum. It is probably the first example of a nonlinear isochrone. For more details see [1].

Isochronicity appears in a wide variety of Physics phenomena and it is also closely related to the uniqueness and existence of solutions for some boundary value, perturbation, or bifurcation problems. Moreover it is important in stability theory, since a periodic solution in the region surrounding the center type singular point is Liapunov stable if and only if the neighboring periodic solutions have the same period. For more details on these topics see [2]. In the last decades the study of isochronous systems has been increased due to the proliferation of powerful methods of computerized research, and special attention has been dedicated to polynomial differential systems, see [3–6] and the bibliography therein.

In this paper we classify the global phase portraits of all quartic polynomial differential systems with a uniform isochronous center at the origin such that their nonlinear part is not homogeneous.

Let $p \in \mathbb{R}^2$ be a center of a differential polynomial system in $\mathbb{R}^2$, without loss of generality we can assume that p is the origin of coordinates. We say that p is an *isochronous center* if it is a center having a neighborhood such that all the periodic orbits in this neighborhood have the same period. We say that p is a *uniform isochronous center* if the system, in polar coordinates $x = r\cos\theta$, $y = r\sin\theta$, takes the form $\dot r = G(\theta, r)$, $\dot\theta = k$, $k \in \mathbb{R} \setminus \{0\}$, for more details see Conti [5].

Proposition 1. *Assume that a planar differential polynomial system $\dot x = P(x, y)$, $\dot y = Q(x, y)$ of degree n has a center at the origin of coordinates. Then, this center is uniform isochronous if and only if by doing a linear change of variables and a rescaling of time it can be written into the form*

$$\dot x = -y + x f(x, y), \qquad \dot y = x + y f(x, y), \tag{1}$$

where $f(x, y)$ is a polynomial in x and y of degree $n - 1$, and $f(0, 0) = 0$.

* Corresponding author. Tel.: +34 93 5811303; fax: +34 935812790.
E-mail addresses: itikawa@mat.uab.cat (J. Itikawa), jllibre@mat.uab.cat (J. Llibre).

http://dx.doi.org/10.1016/j.cam.2015.02.046
0377-0427/

Since we cannot find a proof of the well known Proposition 1 in the literature we have provided a proof in our paper at the beginning of Section 3.

Algaba et al. [7] in 1999, and Chavarriga et al. [8] in 2001, independently provided the following characterization of quartic polynomial systems with an isolated uniform isochronous center at the origin.

Theorem 2. *Consider $f(x, y) = \sum_{i=1}^{3} f_i(x, y)$ where $f_i(x, y)$ for $i = 1, 2, 3$ are homogeneous polynomials of degree i, $f_1^2 + f_2^2 \neq 0$ and $f_3 \neq 0$ such that (1) be a quartic polynomial differential system. Then the only case of local analytic integrability in an open neighborhood of the origin of system (1) is given, modulo a rotation, by the time-reversible system.*

$$\begin{aligned} \dot{x} &= -y + x(A_1x + B_2xy + C_1x^3 + C_3xy^2), \\ \dot{y} &= \ \ x + y(A_1x + B_2xy + C_1x^3 + C_3xy^2), \end{aligned} \tag{2}$$

where $A_1, B_2, C_1, C_3 \in \mathbb{R}$.

By the following classical result due to Poincaré [9] and Liapunov [10] Theorem 2 characterizes the quartic uniform isochronous centers, except the ones for which the polynomial $f(x, y)$ is a homogeneous polynomial of degree 3.

Theorem 3. *An analytic differential system $\dot{x} = -y+F_1(x, y),\ \dot{y} = x+F_2(x, y)$, with $F_1(x, y)$ and $F_2(x, y)$ real analytic functions without constant and linear terms defined in a neighborhood of the origin, has a center at the origin if and only if there exists a local analytic first integral of the form $H = x^2 + y^2 + G(x, y)$ defined in a neighborhood of the origin, where G starts with terms of order higher than two.*

Algaba et al. [7] provided the phase portraits of systems (2) in the particular case $C_1 = 0$. In such case systems (2) have a polynomial commutator, allowing to get the bifurcation diagram of the systems. In Theorem 4, we provide all the global phase portraits of systems (2).

Theorem 4. *Consider a quartic polynomial differential system $X : \mathbb{R}^2 \to \mathbb{R}^2$ and assume that X has a uniform isochronous center at the origin such that their nonlinear part is not homogeneous. Then the global phase portrait of X is topologically equivalent to one of the 14 phase portraits of Fig. 1.*

More precisely, since X can always be written as system (2), the global phase portrait of X is topologically equivalent to the phase portrait

(a) *of Fig. 1 if either $C_1C_3 > 0$, or $C_3 = 0,\ B_2 < 0$;*
(b) *of Fig. 1 if $C_1 = 0,\ C_3 \neq 0$ and if either $r_1, r_2, r_3 > 0$, or $r_1, r_2, r_3 < 0$;*
(c) *of Fig. 1 if $C_1 = 0,\ C_3 \neq 0$ and if either $r_1 < 0, r_2, r_3 > 0$, or $r_1, r_2 < 0, r_3 > 0$;*
(d) *of Fig. 1 if $C_1 = 0,\ C_3 \neq 0$ and if either $r_1r_2 > 0, r_3 = r_2$, or $r_2 = r_1, r_1r_3 > 0$;*
(e) *of Fig. 1 if $C_1 = 0,\ C_3 \neq 0$ and if either $r_1 < 0, r_2 > 0, r_3 = r_2$, or $r_2 = r_1, r_1 < 0, r_3 > 0$;*
(f) *of Fig. 1 if $C_1 = 0,\ C_3 \neq 0$ and if either $r_3 = r_2 = r_1,\ \forall r_1, r_2, r_3 \in \mathbb{R}^*$, or $r_1 \neq 0$ and $r_{2,3} = a \pm bi,\ \forall r_1, b \in \mathbb{R}^*, a \in \mathbb{R}$;*
(g) *of Fig. 1 if $C_3 = 0,\ C_1 \neq 0,\ B_2 > 0,\ C_1 \neq -A_1B_2$;*
(h) *of Fig. 1 if either $C_3 = 0,\ C_1 \neq 0,\ B_2 > 0,\ C_1 = -A_1B_2$, or $B_2 = C_3 = 0$;*
(i) *or* (j) *or* (k) *of Fig. 1 if $C_1C_3 < 0,\ B_2 = 0$;*
(j) *or* (m) *or* (n) *of Fig. 1 if $C_1C_3 < 0,\ B_2 \neq 0$;*

where in the cases with $C_1 = 0$, we have that r_1, r_2, r_3 are the roots of the polynomial $-C_3 - B_2x - A_1x^2 - x^3$ and we assume that $r_1 \leq r_2 \leq r_3$ when these roots are real.

Our results have been checked with the software *P4*, see for more details on this software the Chapters 9 and 10 of [11].

The rest of the paper is organized as follows. In Section 2 we present some results and technical propositions used in our study. In Section 3 we prove Theorem 4.

2. Preliminary results

In this section we present some results necessary to our study.

Poincaré compactification

Let $\mathcal{X}$ be a planar vector field of degree n. The *Poincaré compactified vector field $p(\mathcal{X})$ corresponding to $\mathcal{X}$* is an analytic vector field induced on $\mathbb{S}^2$ as follows (see, for instance [12], or Chapter 5 of [11]). Let $\mathbb{S}^2 = \{y = (y_1, y_2, y_3) \in \mathbb{R}^3 : y_1^2 + y_2^2 + y_3^2 = 1\}$ (the *Poincaré sphere*) and $T_y\mathbb{S}^2$ be the tangent space to $\mathbb{S}^2$ at point y. Consider the central projection $f : T_{(0,0,1)}\mathbb{S}^2 \to \mathbb{S}^2$. This map defines two copies of $\mathcal{X}$, one in the northern hemisphere and the other in the southern hemisphere. Denote by $\mathcal{X}'$ the vector field $Df \circ \mathcal{X}$ defined on $\mathbb{S}^2$ except on its equator $\mathbb{S}^1 = \{y \in \mathbb{S}^2 : y_3 = 0\}$. Clearly $\mathbb{S}^1$ is identified to the *infinity* of $\mathbb{R}^2$. In order to extend $\mathcal{X}'$ to a vector field on $\mathbb{S}^2$ (including $\mathbb{S}^1$) it is necessary that $\mathcal{X}$ satisfies suitable conditions. In the case that $\mathcal{X}$ is a planar vector field of degree n then $p(\mathcal{X})$ is the only analytic extension of $y_3^{n-1}\mathcal{X}'$ to $\mathbb{S}^2$. On $\mathbb{S}^2 \backslash \mathbb{S}^1$

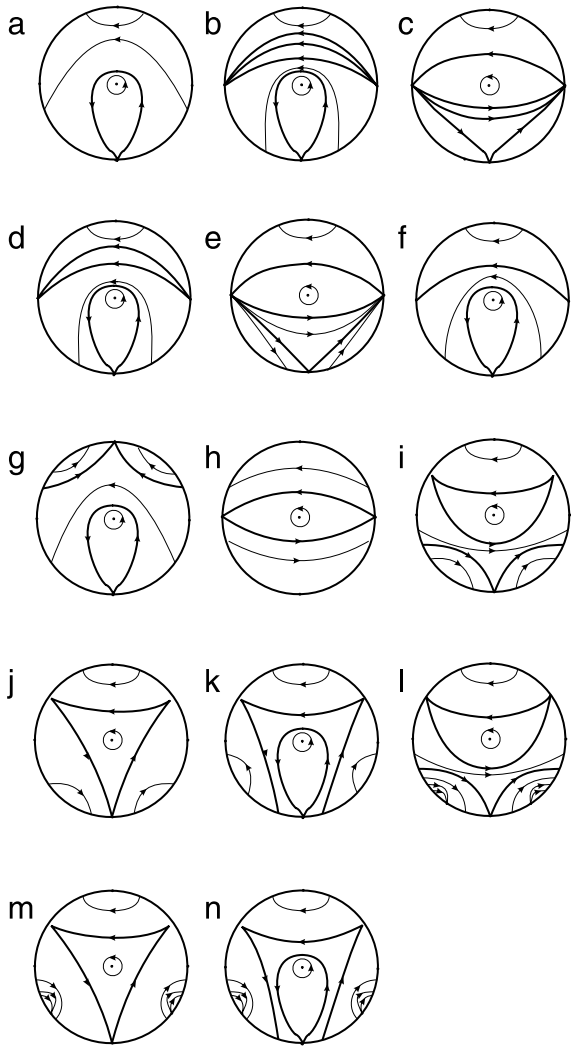

Fig. 1. Phase portraits of the uniform isochronous centers (2) of degree 4 with $f(x, y)$ non homogeneous polynomial.

there are two symmetric copies of $\mathcal{X}$, and knowing the behavior of $p(\mathcal{X})$ around $\mathbb{S}^1$, we know the behavior of $\mathcal{X}$ at infinity. The projection of the closed northern hemisphere of $\mathbb{S}^2$ on $y_3 = 0$ under $(y_1, y_2, y_3) \longmapsto (y_1, y_2)$ is called the *Poincaré disc*, and it is denoted by $\mathbb{D}^2$. The Poincaré compactification has the property that $\mathbb{S}^1$ is invariant under the flow of $p(\mathcal{X})$.

As $\mathbb{S}^2$ is a differentiable manifold, for computing the expression for $p(\mathcal{X})$, we consider the six local charts $U_i = \{y \in \mathbb{S}^2 : y_i > 0\}$, and $V_i = \{y \in \mathbb{S}^2 : y_i < 0\}$ where $i = 1, 2, 3$; and the diffeomorphisms $F_i : U_i \to \mathbb{R}^2$ and $G_i : V_i \to \mathbb{R}^2$ for $i = 1, 2, 3$ are the inverses of the central projections from the planes tangent at the points $(1, 0, 0)$, $(-1, 0, 0)$, $(0, 1, 0)$, $(0, -1, 0)$, $(0, 0, 1)$ and $(0, 0, -1)$ respectively. We denote by $(u,\ v)$ the value of $F_i(y)$ or $G_i(y)$ for any $i = 1, 2, 3$ (so $(u,\ v)$ represents different things according to the local charts under consideration).

The expression for $p(\mathcal{X})$ in the local chart (U_1, F_1) is given by

$$\dot{u} = v^n \left[-uP\left(\frac{1}{v}, \frac{u}{v}\right) + Q\left(\frac{1}{v}, \frac{u}{v}\right)\right], \qquad \dot{v} = -v^{n+1} P\left(\frac{1}{v}, \frac{u}{v}\right).$$

The expression for $p(\mathcal{X})$ in local chart (U_2, F_2) is

$$\dot{u} = v^n \left[P\left(\frac{u}{v}, \frac{1}{v}\right) - uQ\left(\frac{u}{v}, \frac{1}{v}\right)\right], \qquad \dot{v} = -v^{n+1} Q\left(\frac{u}{v}, \frac{1}{v}\right),$$

and for (U_3, F_3) is

$$\dot{u} = P(u, v), \qquad \dot{v} = Q(u, v).$$

The expression for $p(\mathcal{X})$ in the chart (V_i, G_i) is the same than in the chart (U_i, F_i) multiplied by $(-1)^{n-1}$ for $i = 1,\ 2,\ 3$. The points of $\mathbb{S}^1$ in any chart have $v = 0$. Thus we obtain a polynomial vector field in each local chart.

Since the unique singular points at infinity which cannot be contained into the charts $U_1 \cup V_1$ are the origins of U_2 and V_2, when we study the infinite singular points on the charts $U_2 \cup V_2$, we only need to verify if the origin of these charts are singular points.

Topological equivalence

We say that two polynomial vector fields X and Y on $\mathbb{R}^2$ are *topologically equivalent* if there exists a homeomorphism on $\mathbb{S}^2$ preserving the infinity $\mathbb{S}^1$ carrying orbits of the flow induced by $p(X)$ into orbits of the flow induced by $p(Y)$, preserving or reversing simultaneously the sense of all orbits.

A *separatrix* of $p(X)$ is an orbit which is either a singular point, or a limit cycle, or a trajectory which lies in the boundary of a hyperbolic sector at a singular point, finite or infinity.

We denote by $\mathrm{Sep}(p(X))$ the set formed by all separatrices of $p(X)$. Neumann [13] proved that the set $\mathrm{Sep}(p(X))$ is closed. Each open connected component of $\mathbb{S}^2 \setminus \mathrm{Sep}(p(X))$ is called a *canonical region* of $p(X)$. A *separatrix configuration* is defined as a union of $\mathrm{Sep}(p(X))$ plus one representative solution chosen from each canonical region. We say that $\mathrm{Sep}(p(X))$ and $\mathrm{Sep}(p(Y))$ are *equivalent* if there exists a homeomorphism in $\mathbb{S}^2$ preserving the infinity $\mathbb{S}^1$ carrying orbits of $\mathrm{Sep}(p(X))$ into orbits of $\mathrm{Sep}(p(Y))$, preserving or reversing simultaneously the sense of all orbits.

The next result is due to Neumann [13] and characterizes the topologically equivalence between two Poincaré compactified vector fields.

Theorem 5. *Suppose that $p(X)$ and $p(Y)$ are two continuous flows in $\mathbb{S}^2$ with finitely many separatrices. Then $p(X)$ and $p(Y)$ are topologically equivalent if and only if their separatrix configurations are equivalent.*

Theorem 5 implies that, in order to obtain the global phase portrait of a polynomial vector field $p(X)$ with finitely many separatrices, we essentially need to determine the α- and the ω-limit sets of all separatrices of $p(X)$.

Theorem 6. *If $p(X)$ and $p(Y)$ have the infinity filled of singular points and finitely many separatrices in $\mathbb{R}^2$, we shall work with X and Y. Then X and Y are topologically equivalent if and only if their separatrix configurations are equivalent.*

Theorem 6 implies that, in order to obtain the global phase portrait of a polynomial vector field X with the infinity filled of singular points and finitely many finite singular points, we essentially need to determine the α- and the ω-limit sets of all separatrices of X.

3. Proof of the results

Proof of Proposition 1. Using blow up techniques we know that neither nilpotent nor degenerate centers can have uniform isochronous centers. This is due to the fact that, after the blow up, nilpotent and degenerate centers become a graphic, and the periodic orbits of those centers tending to the graphic have period tending to the infinity, and thus, the period cannot be constant. Hence, only systems having linear-type centers can have a uniform isochronous center at the origin

$$\begin{aligned} \dot{x} &= -y + p(x, y), \\ \dot{y} &= \ \ x + q(x, y), \end{aligned}$$

where $p(x, y)$ and $q(x, y)$ are polynomials starting with at least terms of second order.

By doing a polar change of coordinates in this system, we have

$$\begin{aligned} \dot{r} &= \left. \frac{x\, p(x, y) + y\, q(x, y)}{\sqrt{x^2 + y^2}} \right|_{(x,y)=(r\cos\theta, r\sin\theta)}, \\ \dot{\theta} &= 1 + \left. \frac{x\, q(x, y) - y\, p(x, y)}{x^2 + y^2} \right|_{(x,y)=(r\cos\theta, r\sin\theta)}. \end{aligned} \tag{3}$$

But by hypothesis, system (3) has a uniform isochronous center at the origin, that is, $\dot{\theta} = 1$. Hence, $x\, q(x, y) - y\, p(x, y) = 0$, and thus

$$\begin{aligned} p(x, y) &= x\, f(x, y), \\ q(x, y) &= y\, f(x, y), \end{aligned}$$

where $f(x, y)$ is a polynomial.

Reciprocally, if a polynomial differential system is of the form (1), then by doing a polar change of coordinates we obtain

$$\begin{aligned} \dot{r} &= r\, f(r\cos\theta, r\sin\theta), \\ \dot{\theta} &= 1. \end{aligned} \tag{4}$$

Hence, it has a uniform isochronous center at the origin. □

For providing all the possible phase portraits in the Poincaré disc for the planar quartic polynomial differential systems with a uniform isochronous center at the origin such that their nonlinear part is not homogeneous, we shall start studying all the finite and infinite singular points of such systems. We remark that in this work we never consider the quartic polynomial differential systems (1) with a uniform isochronous center such that $f(x, y)$ is a homogeneous polynomial.

By Theorem 2 a planar quartic polynomial differential system with a uniform isochronous center at the origin always can be written as a system (2). These systems are invariant under the transformation $(x, y, t) \mapsto (-x, y, -t)$, and therefore, all their phase portraits are symmetric respect to the y-axis.

3.1. Finite singular points

In polar coordinates (r, θ) defined by $(x, y) = (r\cos\theta, r\sin\theta)$ a planar differential system with a uniform isochronous center at the origin (2) always can be written as $\dot r = P(r, \theta),\ \dot\theta = 1$. Hence such systems have no finite singular points except the origin.

The *period annulus* of a center is the biggest punctured neighborhood only foliated by periodic orbits. Compactifying $\mathbb{R}^2$ to the Poincaré disc, the boundary of the period annulus of a center has two connected components: the center itself and a graphic. Since the origin is the only finite singular point in the systems we are interested to study, the graphic of the period annulus of uniform isochronous center cannot present finite singularities. Hence, such a graphic shall be formed either by infinite singular points and separatrices of these infinite singular points, or by the periodic solution at infinity when at infinity there are no singular points.

3.2. Infinite singular points

In the chart U_1 the differential system (2) becomes

$$\begin{aligned} \dot u &= (1+u^2)v^3,\\ \dot v &= (-C_1 - C_3u^2 - B_2uv - A_1v^2 + uv^3)v, \end{aligned} \tag{5}$$

and therefore all the points $(u, 0)$ for all $u \in \mathbb{R}$ are infinite singular points of the differential system (2) in U_1. In order to obtain the local phase portraits at these points, after the rescaling of time $ds = vdt$ system (5) becomes

$$\begin{aligned} u' &= (1+u^2)v^2,\\ v' &= -C_1 - C_3u^2 + v(-B_2u - A_1v + uv^2), \end{aligned} \tag{6}$$

where the prime denotes derivative with respect to s.

In chart U_2, system (2) becomes

$$\begin{aligned} \dot u &= -(1+u^2)v^3,\\ \dot v &= (-C_3u - C_1u^3 - B_2uv - A_1uv^2 - uv^3)v. \end{aligned} \tag{7}$$

We only need to study the point $(0, 0)$ of U_2. Doing the rescaling of time $ds = vdt$, we obtain the system

$$\begin{aligned} u' &= -(1+u^2)v^2,\\ v' &= -C_3u - C_1u^3 - B_2uv - A_1uv^2 - uv^3. \end{aligned} \tag{8}$$

We shall apply the well known results for the hyperbolic, semi-hyperbolic and nilpotent singular points, see for instance Theorems 2.15, 2.19 and 3.15 of [11], for the characterization of the local phase portraits at each singular point of systems (6) and (8).

Case I: $\mathbf{C_1 = 0}$. We remark that if $C_1 = C_3 = 0$ system (2) degenerates to a cubic polynomial differential system, whose global phase portraits are well known, see for instance [14]. Therefore in Case I we assume $C_3 \neq 0$.

We first analyze the chart U_2. We denote by O_{U_2} the origin of the chart U_2. The corresponding linear part of system (8) at O_{U_2} is

$$\begin{pmatrix} 0 & 0\\ -C_3 & 0 \end{pmatrix}.$$

Therefore O_{U_2} is a nilpotent singularity and applying Theorem 3.5 of [11] we conclude that it is a cusp, whose behavior depends on the sign of the coefficient C_3. Hence, the local phase portrait at the origin for system (8) might be one of the two shown in Fig. 2.

We now perform the study for the chart U_1. Clearly the only singular point at infinity in the chart U_1 is the origin, which we denote by O_{U_1}.

The corresponding linear part of system (6) at O_{U_1} is identically zero. So it is necessary to apply a directional blow up $(u, v) \mapsto (u, w)$ where $v = uw$, and we obtain the system

$$\begin{aligned} u' &= (1+u^2)u^2w^2,\\ w' &= u(-C_3 - B_2w - A_1w^2 - w^3). \end{aligned} \tag{9}$$

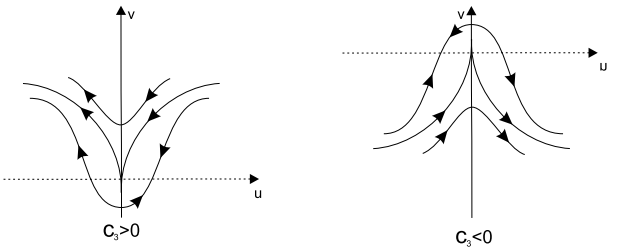

Fig. 2. Local phase portrait at the origin of system (7). The horizontal axis is filled with singular points.

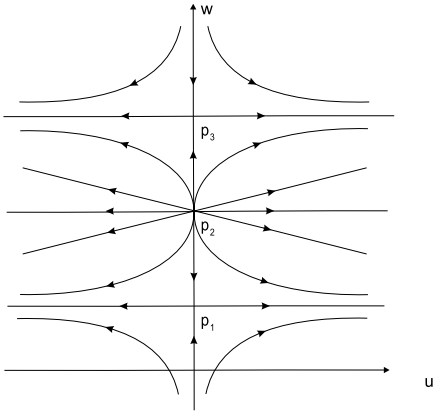

Fig. 3. Phase portrait of system (10) for $0 < r_1 < r_2 < r_3$.

Performing a change of the independent variable of the form $dT = u\,ds$ in system (9), we get the system

$$\begin{aligned} u' &= (1+u^2)uw^2, \\ w' &= -C_3 - B_2 w - A_1 w^2 - w^3, \end{aligned} \tag{10}$$

where the prime now denotes derivative with respect to T. The singular points of system (10) are of the form $(0, r_i)$, $i = 1, 2, 3$, where r_1, r_2, r_3 are the roots of the polynomial $-C_3 - B_2 w - A_1 w^2 - w^3$, that is, $A_1 = -(r_1 + r_2 + r_3)$, $B_2 = r_1 r_2 + r_1 r_3 + r_2 r_3$, $C_3 = -r_1 r_2 r_3$. We observe that, since we are assuming $C_3 \neq 0$, we have $r_1 r_2 r_3 \neq 0$. Hence, we have the following cases. Of course, of these roots we only need to take into account the real ones.

Subcase I.1: **Three simple real roots**. Without loss of generality we assume that $r_1 < r_2 < r_3$. The singular points at the infinity are $p_1 = (0, r_1)$, $p_2 = (0, r_2)$, and $p_3 = (0, r_3)$. The corresponding linear part of system (10) at each of these points is respectively

$$\begin{pmatrix} r_1^2 & 0 \\ 0 & -(r_1 - r_2)(r_1 - r_3) \end{pmatrix}, \quad \begin{pmatrix} r_2^2 & 0 \\ 0 & (r_1 - r_2)(r_2 - r_3) \end{pmatrix}, \quad \begin{pmatrix} r_3^2 & 0 \\ 0 & -(r_1 - r_3)(r_2 - r_3) \end{pmatrix}.$$

Applying Theorem 2.15 of [11] and the hypotheses $r_1 < r_2 < r_3$, $r_1 r_2 r_3 \neq 0$ in the above expressions we conclude that p_1 and p_3 are saddles, and p_2 is an unstable node. The resulting singularity obtained from the blow down of p_1, p_2 and p_3 depends on the position of these singular points with respect to the origin of the u-axis. Hence we have the following subcases.

Subcase I.1.1: $\mathbf{0 < r_1 < r_2 < r_3}$. The local phase portraits at the singularities p_i, $i = 1, 2, 3$ for system (10) and system (9) are shown in Figs. 3 and 4, respectively.

Going back through the blow up we get the local phase portrait at the origin of system (6), see Fig. 5. Finally, taking into account the rescaling of time $ds = v dt$, we obtain that the phase portrait at the origin of system (5) is topologically equivalent to the one of Fig. 6.

For the chart U_2, since $r_1, r_2, r_3 > 0$ then $C_3 = -r_1 r_2 r_3 < 0$, and we obtain a local phase portrait as the one in Fig. 2 ($C_3 < 0$).

In short, the global phase portrait in this case is obtained taking into account all the local phase portraits of the finite and infinite singular points, the existence and uniqueness theorem for the solutions of a differential system, the fact that all the phase portraits of planar quartic polynomial differential systems with a uniform isochronous center at the origin are symmetric with respect to the y-axis, and that the graphic at the boundary of the period annulus of the uniform isochronous center at the origin is formed by separatrices of infinite singular points. Hence we obtain that the global phase portrait for Subcase I.1.1 is topologically equivalent to the one of Fig. 1(b) of Theorem 4.

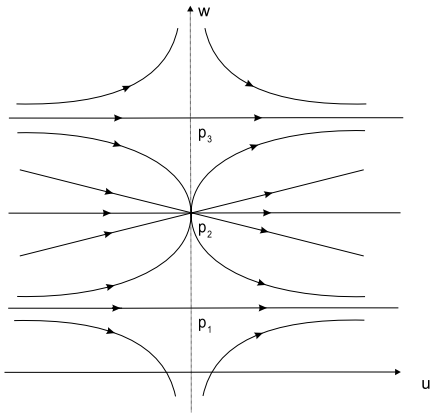

Fig. 4. Phase portrait of system (9) for $0 < r_1 < r_2 < r_3$. The vertical axis is filled of singular points.

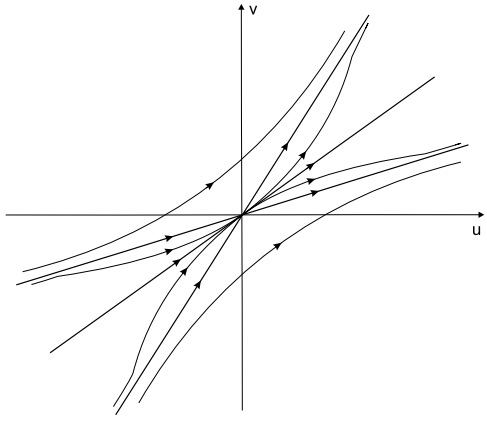

Fig. 5. Phase portrait of system (6) for $0 < r_1 < r_2 < r_3$.

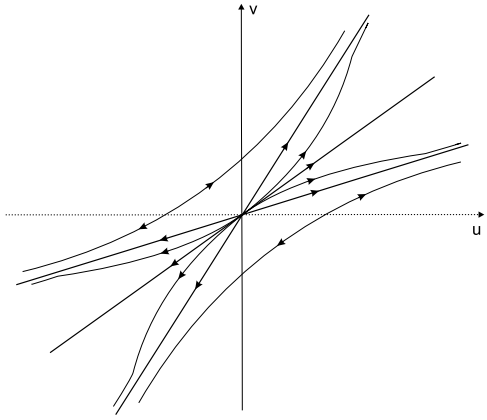

Fig. 6. Phase portrait of system (5) for $0 < r_1 < r_2 < r_3$. The horizontal axis is filled of singular points.

Subcase I.1.2: $\mathbf{r_1 < 0 < r_2 < r_3}$. The resulting local phase portrait at the origin of system (5) is given in Fig. 7. This local phase portrait is obtained proceeding in a similar way to Case I.1.1.

For the chart U_2, since $r_1 < 0$ and $r_2, r_3 > 0$ then $C_3 = -r_1 r_2 r_3 > 0$ and we have a local phase portrait topologically equivalent to the one of Fig. 2 ($C_3 > 0$). Therefore the global phase portrait for Subcase I.1.2 is shown in Fig. 1(c) of Theorem 4.

Subcase I.1.3: $\mathbf{r_1 < r_2 < 0 < r_3}$. The phase portrait at the origin of system (5) is given in Fig. 8. This local phase portrait is obtained proceeding in a similar way to Case I.1.1.

For the chart U_2, since $C_3 = -r_1 r_2 r_3 < 0$, we have a local phase portrait topologically equivalent to the one of Fig. 2 ($C_3 < 0$). Then the global phase portrait for Subcase I.1.3 is shown in Fig. 1(c) of Theorem 4.

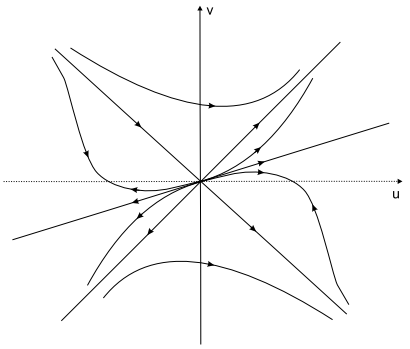

Fig. 7. Phase portrait of system (5) for $r_1 < 0 < r_2 < r_3$.

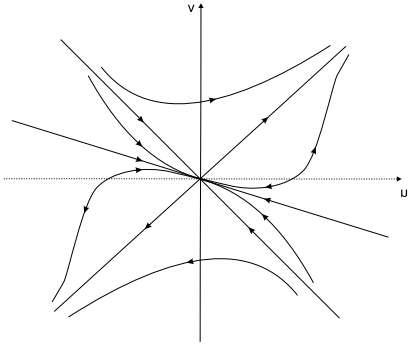

Fig. 8. Phase portrait of system (5) for $r_1 < r_2 < 0 < r_3$.

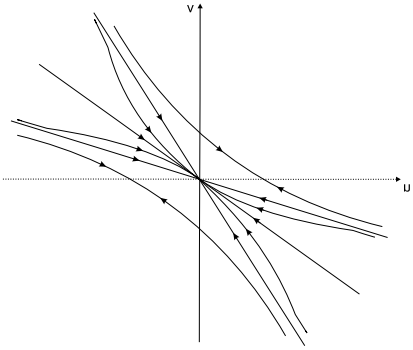

Fig. 9. Phase portrait of system (5) for $r_1 < r_2 < r_3 < 0$.

Subcase I.1.4: $\mathbf{r_1 < r_2 < r_3 < 0}$. The resulting phase portrait at the origin of system (5) is given in Fig. 9, obtained as in case I.1.1.

For the chart U_2, since $C_3 = -r_1r_2r_3 > 0$, we have a local phase portrait topologically equivalent to the one of Fig. 2 ($C_3 > 0$). So the global phase portrait for Subcase I.1.3 is shown in Fig. 1(b) of Theorem 4.

Subcase I.2: **One simple real root and one double real root**. Without loss of generality we consider two distinct cases depending on the relative position of the simple and the double real roots: $r_1 < r_2 = r_3$ and $r_1 = r_2 < r_3$. We start with the first case. The singular points at infinity are $p_1 = (0, r_1)$ and $p_2 = (0, r_2)$. The corresponding linear part of system (10) at each of these points is respectively

$$\begin{pmatrix} r_1^2 & 0 \\ 0 & -(r_1 - r_2)^2 \end{pmatrix} \quad \text{and} \quad \begin{pmatrix} r_2^2 & 0 \\ 0 & 0 \end{pmatrix}.$$

Now we assume $\mathbf{r_1 < r_2 = r_3}$, and $r_1, r_2 \neq 0$ in the above expressions and applying Theorems 2.15, 2.19 of [11], we conclude that p_1 is a saddle and p_2 is a saddle–node. The resulting singularity obtained from the blow down of p_1 and p_2 depends on the position of such singular points with respect to the horizontal axis. Hence we have the following cases.

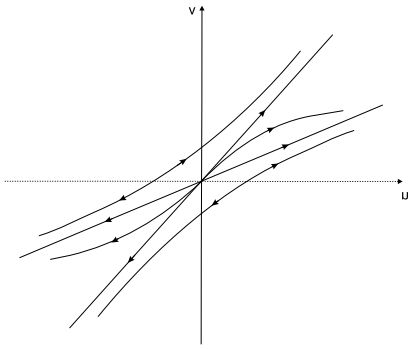

Fig. 10. Phase portrait of system (5) for $0 < r_1 < r_2 = r_3$.

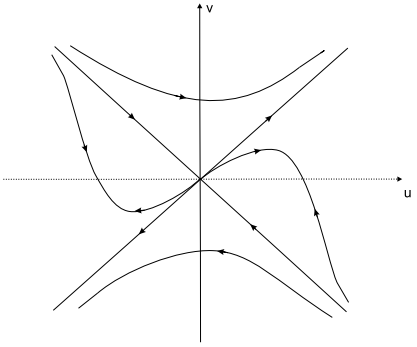

Fig. 11. Phase portrait of system (5) for $r_1 < 0 < r_2 = r_3$.

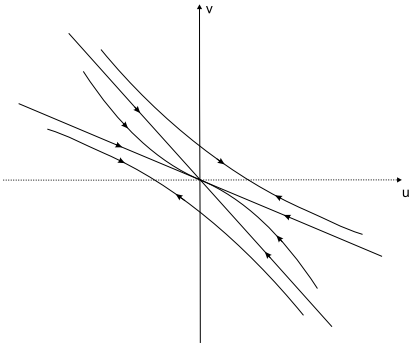

Fig. 12. Phase portrait of system (5) for $r_1 < r_2 = r_3 < 0$.

Subcase I.2.1: $\mathbf{0 < r_1 < r_2}$. In this case the local phase portrait at the origin of system (5) is given in Fig. 10, obtained as in case I.1.1.

For the chart U_2, since $C_3 = -r_1 r_2^2 < 0$, we have a local phase portrait similar to the one in Fig. 2 ($C_3 < 0$). Consequently the global phase portrait for Subcase I.2.1 is shown in Fig. 1(d) of Theorem 4.

Subcase I.2.2: $\mathbf{r_1 < 0 < r_2}$. The local phase portrait at the origin of system (5) is given in Fig. 11, obtained as in case I.1.1.

For the chart U_2, since $C_3 = -r_1 r_2^2 > 0$, we have a local phase portrait topologically equivalent to the one of Fig. 2 ($C_3 > 0$), and the global phase portrait for Subcase I.2.2 is shown in Fig. 1(e) of Theorem 4.

Subcase I.2.3: $\mathbf{r_1 < r_2 < 0}$. The resulting phase portrait at the origin of system (5) is given in Fig. 12. This local phase portrait is obtained proceeding in a similar way to the case I.1.1.

For the chart U_2, since $C_3 = -r_1 r_2^2 > 0$, we have a local phase portrait topologically equivalent to the one of Fig. 2 ($C_3 > 0$).

The resulting global phase portrait for Subcase I.2.3 is shown in Fig. 1(d) of Theorem 4.

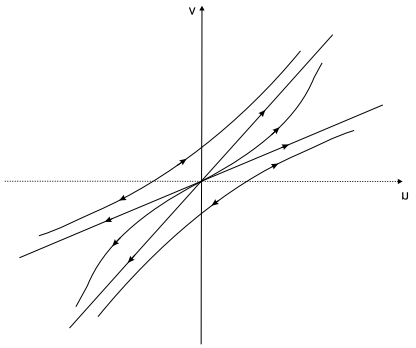

Fig. 13. Phase portrait of system (5) for $0 < r_1 = r_2 < r_3$.

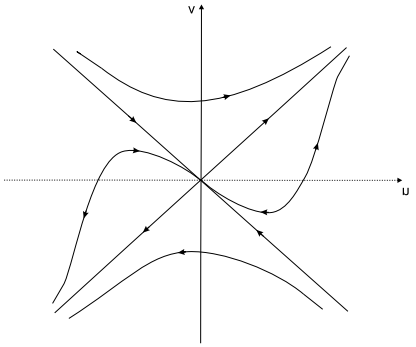

Fig. 14. Phase portrait of system (5) for $r_1 = r_2 < 0 < r_3$.

Now we analyze the case $\mathbf{r_1 = r_2 < r_3}$. The singular points at the infinity are $p_1 = (0, r_1), p_2 = (0, r_3)$. The corresponding linear part of system (10) at each of these points is respectively

$$\begin{pmatrix} r_1^2 & 0 \\ 0 & 0 \end{pmatrix}, \qquad \begin{pmatrix} r_3^2 & 0 \\ 0 & -(r_1 - r_3)^2 \end{pmatrix}.$$

Considering that we assume $r_1 < r_3$, and $r_1, r_3 \neq 0$ in the above expressions and applying Theorems 2.15 and 2.19 of [11], we conclude that p_1 is a saddle–node, and p_2 is a saddle. The resulting singularity obtained from the blow down of p_1, and p_2 depends on the position of such singular points to the horizontal axis. Hence, we have the following cases.

Subcase I.2.4: $\mathbf{0 < r_1 < r_3}$. In this case the local phase portrait at the origin of system (5) is given in Fig. 13, obtained as in case I.1.1.

We remark that the dynamics in the above phase portrait is almost topologically equivalent to the one of Case I.2.1, except between the two separatrices.

For the chart U_2, since $C_3 = -r_1^2 r_3 < 0$, we have a local phase portrait topologically equivalent to the one of Fig. 2 ($C_3 < 0$). Then the global phase portrait for Subcase I.2.4 is shown in Fig. 1(d) of Theorem 4.

Subcase I.2.5: $\mathbf{r_1 < 0 < r_3}$. In this case the local phase portrait at the origin of system (5) is given in Fig. 14.

For the chart U_2, since $C_3 = -r_1^2 r_3 < 0$, we have a local phase portrait topologically equivalent to the one of Fig. 2 ($C_3 < 0$). Hence the global phase portrait for Subcase I.2.5 is shown in Fig. 1(e) of Theorem 4.

Subcase I.2.6: $\mathbf{r_1 < r_3 < 0}$. In this case the local phase portrait at the origin of system (5) is given in Fig. 15.

We remark that the dynamics in the above phase portrait is almost topologically equivalent to the one of Case I.2.1, except between the two separatrices.

For the chart U_2, since $C_3 = -r_1^2 r_3 > 0$, we have a local phase portrait topologically equivalent to the one of Fig. 2 ($C_3 > 0$). Therefore the global phase portrait for Subcase I.2.6 is shown in Fig. 1(d) of Theorem 4.

Subcase I.3: **One triple real root**. In this case we have $r_1 = r_2 = r_3$. Hence the only singular point at infinity is $p_1 = (0, r_1)$. The corresponding linear part of system (10) at p_1 is

$$\begin{pmatrix} r_1^2 & 0 \\ 0 & 0 \end{pmatrix}.$$

Since $r_1 \neq 0$ from Theorem 2.19 of [11], it follows that p_1 is a saddle. Then the resulting singularity obtained from the blow down of p_1 depends on the position of such singular point with respect to the horizontal axis. So we distinguish the following cases.

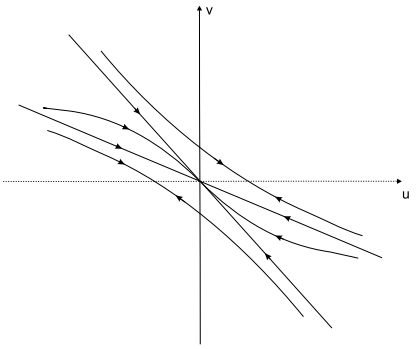

Fig. 15. Phase portrait of system (5) for $r_1 = r_2 < r_3 < 0$.

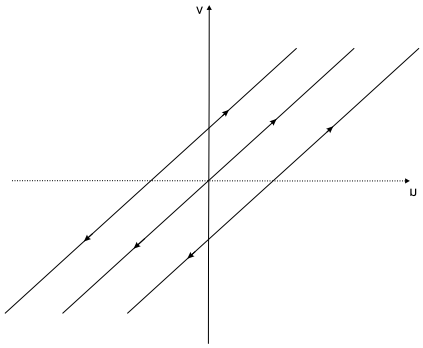

Fig. 16. Phase portrait of system (5) for $0 < r_1 = r_2 = r_3$.

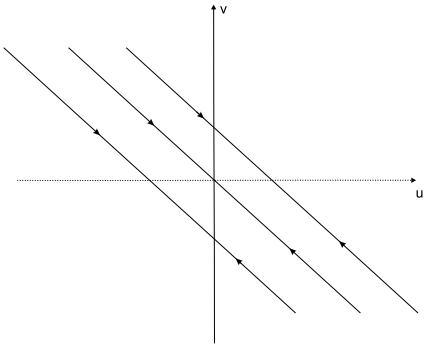

Fig. 17. Phase portrait of system (5) for $r_3 = r_2 = r_1 < 0$.

Subcase I.3.1: $\mathbf{r_1 > 0}$. In this case the local phase portrait at the origin of system (5) is given in Fig. 16.

For the chart U_2, since $C_3 = -r_1^3 < 0$, we have a local phase portrait topologically equivalent to the one of Fig. 2 ($C_3 < 0$). So the global phase portrait for Subcase I.3.1 is shown in Fig. 1(f) of Theorem 4.

Subcase I.3.2: $\mathbf{r_1 < 0}$. In this case the local phase portrait at the origin of system (5) is given in Fig. 17.

For the chart U_2, since $C_3 = -r_1^3 > 0$, we have a local phase portrait topologically equivalent to the one of Fig. 2 ($C_3 > 0$). Then the global phase portrait for Subcase I.3.2 is shown in Fig. 1(f) of Theorem 4.

Subcase I.4: **One simple real root and two complex conjugate roots**. We denote the real root as r_1 and the two complex conjugate roots as $r_{2,3} = a \pm ib$. Note that, if at least one of the roots r_i, $i = 1, 2, 3$ is zero, we have $C_3 = -r_1(a^2 + b^2) = 0$ and as already commented, the case $C_1 = C_3 = 0$ leads to a cubic polynomial differential system, which has already been studied. Since we are only interested in analyzing the quartic systems, we assume $C_3 \neq 0$, which leads to $r_1, b \neq 0$.

The unique real singular point at infinity is $p_1 = (0, r_1)$. The linear part of system (10) at p_1 is

$$\begin{pmatrix} r_1^2 & 0 \\ 0 & -(b^2 + (a - r_1)^2) \end{pmatrix}.$$

Since $r_1, b \neq 0$ by Theorem 2.15 of [11], we get that p_1 is a saddle. Then the singularity obtained from the blow down of p_1 depends on the position of such singular point with respect to the horizontal axis. So we have the following cases.

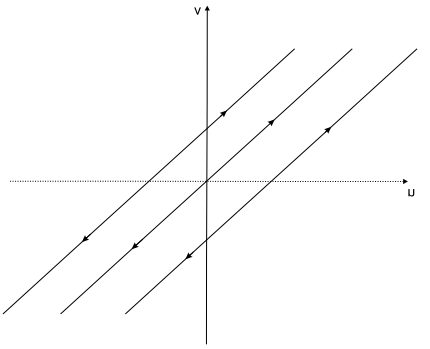

Fig. 18. Phase portrait of system (5) for $r_1 > 0$, $r_{2,3} = a \pm ib$.

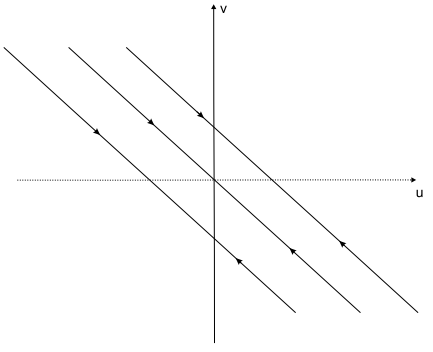

Fig. 19. Phase portrait of system (5) for $r_1 < 0$, $r_{2,3} = a \pm ib$.

Subcase I.4.1: $\mathbf{r_1 > 0}$. In this case the local phase portrait at the origin of system (5) is given in Fig. 18.

For the chart U_2, since $C_3 = -r_1(a^2 + b^2) < 0$, we have a local phase portrait topologically equivalent to the one of Fig. 2 ($C_3 < 0$). Therefore the resulting global phase portrait for Subcase I.4.1 is shown in Fig. 1(f) of Theorem 4.

Subcase I.4.2: $\mathbf{r_1 < 0}$. In this case the local phase portrait at the origin of system (5) is given in Fig. 19.

For the chart U_2, since $C_3 = -r_1(a^2 + b^2) > 0$, we have a local phase portrait topologically equivalent to the one of Fig. 2 ($C_3 > 0$), and the global phase portrait for Subcase I.4.2 is shown in Fig. 1(f) of Theorem 4.

Case II: $\mathbf{C_3 = 0}$. We assume $C_1 \neq 0$ since otherwise system (2) becomes a cubic differential system.

We first study the chart U_1. Then system (6) in this chart becomes

$$\begin{aligned} u' &= (1 + u^2)v^2, \\ v' &= -C_1 - B_2uv - A_1v^2 + uv^3. \end{aligned} \tag{11}$$

Analyzing system (11) we obtain that there is no singular point at infinity in the chart U_1.

For the chart U_2 we only need to study the origin O_{U_2}. The system (8) in that chart writes

$$\begin{aligned} u' &= -(1 + u^2)v^2, \\ v' &= -C_1u^3 - B_2uv - A_1uv^2 - uv^3, \end{aligned} \tag{12}$$

The linear part of system (12) at O_{U_2} is identically zero. Thus it is necessary to apply a directional blow up $v = uw$ to it, resulting the following system

$$\begin{aligned} u' &= -(1 + u^2)u^2w^2, \\ v' &= u(-C_1u - B_2w - A_1uw^2 + w^3). \end{aligned} \tag{13}$$

Doing the rescaling of time $dT = uds$ in system (13) and we get

$$\begin{aligned} u' &= -(1 + u^2)uw^2, \\ v' &= -C_1u - B_2w - A_1uw^2 + w^3, \end{aligned} \tag{14}$$

where the prime now denotes derivative with respect to T. The singular points of system (14) are $p_1 = (0, 0)$, $p_2 = (0, -\sqrt{B_2})$ and $p_3 = (0, \sqrt{B_2})$. Hence we consider the following cases.

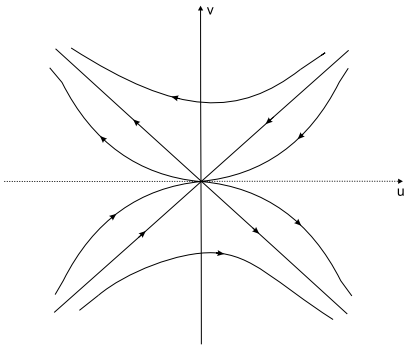

Fig. 20. Phase portrait of system (7) for $B_2 > 0$.

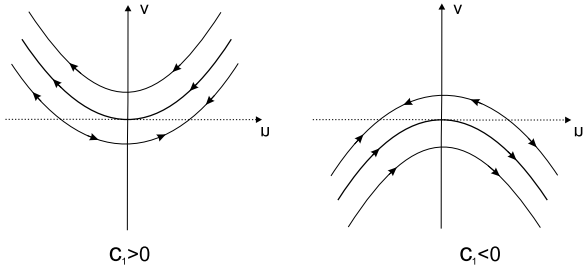

Fig. 21. Phase portrait of system (7) for $B_2 < 0$.

Subcase II.1: $\mathbf{B_2 > 0}$. We have p_1, p_2, p_3 as three distinct real singular points. The corresponding linear part of system (14) at p_1 is

$$\begin{pmatrix} 0 & 0 \\ -C_1 & -B_2 \end{pmatrix}.$$

Applying Theorem 2.19 of [11] we conclude that p_1 is an unstable node.

The linear parts of system (14) at p_2 and p_3 are identical, namely

$$\begin{pmatrix} -B_2 & 0 \\ -A_1B_2 - C_1 & 2B_2 \end{pmatrix}.$$

Applying Theorem 2.15 of [11] it follows that p_2 and p_3 are saddles. Going back with the blow down we get the local phase portrait at the origin of system (7) topologically equivalent to the one of Fig. 20.

We remark that, as it was mentioned, all global phase portraits of planar quartic polynomial differential systems with a uniform isochronous center at the origin are symmetric with respect to the y-axis. Moreover, the graphic at the boundary of the period annulus of the uniform isochronous center at the origin is formed by separatrices of infinite singular points. Considering these results and the above calculations above, we shall have two distinct global phase portraits for Subcase II.1.

Subcase II.1.1: $\mathbf{C_1 = -A_1B_2}$. Under this hypothesis we have the following result.

Lemma 7 (*Invariant Straight Lines*). *If $B_2 > 0$, $C_1 = -A_1B_2$ and $C_3 = 0$ in the quartic polynomial differential system (2) of Theorem 2, then the system has the two invariant straight lines $x = \pm\sqrt{1/B_2}$.*

Proof. If $B_2 > 0, C_1 = -A_1B_2$ and $C_3 = 0$ in system (2), then it writes $\dot{x} = (B_2x^2 - 1)(-A_1x^2 + y), \dot{y} = x(1 + A_1y - A_1B_2x^2y + B_2y^2)$. Hence $x = \pm\sqrt{1/B_2}$ are invariant. □

Using this information we obtain easily the global phase portrait for Subcase II.1.1 shown in Fig. 1(h) of Theorem 4.

Subcase II.1.2: $\mathbf{C_1 \neq -A_1B_2}$. Then the global phase portrait is shown in Fig. 1(g) of Theorem 4.

Subcase II.2: $\mathbf{B_2 < 0}$. The only real singular point is the origin, $p_1 = (0, 0)$. The linear part of system (14) at p_1 is

$$\begin{pmatrix} 0 & 0 \\ -C_1 & -B_2 \end{pmatrix}.$$

Applying Theorem 2.19 of [11] we conclude that p_1 is a saddle.

The local phase portrait at the origin of system (7) depends on the sign of the coefficient C_1 as shown in Fig. 21, obtained as in case I.1.1.

Although the system might present two distinct local phase portraits at the origin, the corresponding global phase portraits are topologically equivalent, and it is shown in Fig. 1(a) of Theorem 4.

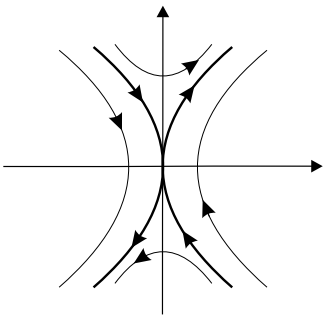

Fig. 22. Saddle of a nilpotent singularity.

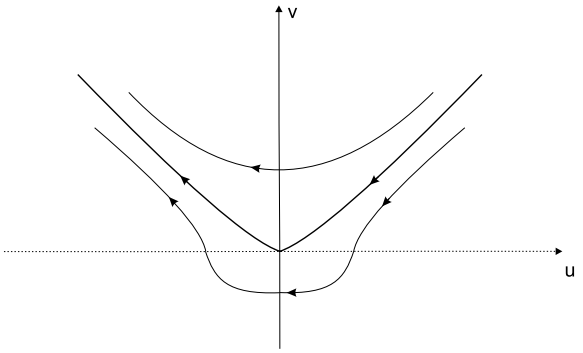

Fig. 23. Phase portrait of system (7) for $C_3 = B_2 = 0$.

Subcase II.3: $\mathbf{B_2 = 0}$. The only singular point is the origin, $p_1 = (0, 0)$. The linear part of system (14) at p_1 is

$$\begin{pmatrix} 0 & 0 \\ -C_1 & 0 \end{pmatrix}.$$

Therefore p_1 is a nilpotent singular point. Applying Theorem 3.5 of [11], we conclude that p_1 is a saddle, similar to the one illustrated in Fig. 22.

The local phase portrait at the origin of system (7) in this case is given in Fig. 23. Then the global phase portrait is shown in Fig. 1(h) of Theorem 4.

Case III: $\mathbf{C_1C_3 > 0}$. There are only two possible singular points in the chart U_1, $(-\sqrt{-C_1/C_3}, 0)$ and $(\sqrt{-C_1/C_3}, 0)$. Since $C_1C_3 > 0$ system (6) in U_1 has no real singular points.

In the chart U_2 the origin, which we denote by O_{U_2} is the only real singular point of system (8). Its linear part is

$$\begin{pmatrix} 0 & 0 \\ -C_3 & 0 \end{pmatrix}.$$

Therefore O_{U_2} is a nilpotent singularity and by Theorem 3.5 of [11] it is a cusp, whose behavior depends on the sign of the coefficient C_3. Hence the local phase portrait at the origin for system (7) might be one of the two shown in Fig. 2. Then the global phase portrait is shown in Fig. 1(a) of Theorem 4.

Case IV: $\mathbf{B_2 = 0}$, $\mathbf{C_1C_3 < 0}$. The expression (6) for the system in the local chart U_1 is

$$\begin{aligned} u' &= (1 + u^2)v^2, \\ v' &= -C_1 - C_3u^2 - A_1v^2 + uv^3. \end{aligned} \tag{15}$$

So there are two singular points at infinity in U_1: $p_1 = (\sqrt{-C_1/C_3}, 0)$ and $p_2 = (-\sqrt{-C_1/C_3}, 0)$. Similarly in the chart U_2 the origin O_{U_2} is a singularity, because the system in that chart is

$$\begin{aligned} u' &= -(1 + u^2)v^2, \\ v' &= -C_3u - C_1u^3 - A_1uv^2 - uv^3. \end{aligned} \tag{16}$$

The linear parts of system (15) at p_1 and p_2, and of system (16) at O_{U_2} are

$$\begin{pmatrix} 0 & 0 \\ -2C_3\sqrt{-C_1/C_3} & 0 \end{pmatrix}, \quad \begin{pmatrix} 0 & 0 \\ 2C_3\sqrt{-C_1/C_3} & 0 \end{pmatrix}, \quad \begin{pmatrix} 0 & 0 \\ -C_3 & 0 \end{pmatrix},$$

respectively.

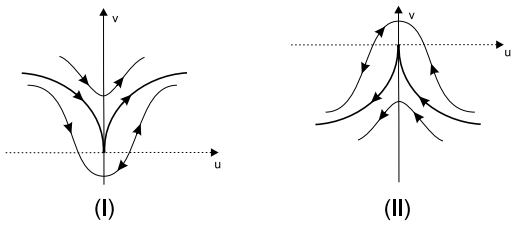

Fig. 24. Phase portrait of system (7) for $B_2 = 0$ and $c_1C_3 < 0$.

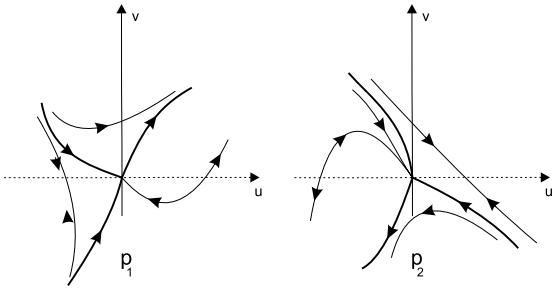

Fig. 25. Phase portrait of system (5) for $A_1, C_1 > 0,\ B_2, C_3 < 0$.

The point O_{U_2} in the chart U_2 is a nilpotent singularity and by Theorem 3.5 of [11] it is a cusp, whose local phase portrait depends on the sign of the coefficient C_3. Hence the local phase portrait at the origin for system (7) might be one of the two shown in Fig. 2.

Since both p_1 and p_2 are also nilpotent singularities we apply the same theorem to determine that p_1 and p_2 are cusps, whose behavior also depends on the sign of C_3, but are slightly distinct from that one of O_{U_2}. For $C_3 < 0$ the local phase portraits at p_1 and p_2 are topologically equivalent to Fig. 24(I) and (II) respectively, whereas for $C_3 > 0$, the local phase portraits at p_1 and p_2 are topologically equivalent to Fig. 24(II) and (I), respectively.

Using similar arguments as in the previous cases, we shall have three possible configurations for the global phase portraits, they are shown in Fig. 1(i), (j) and (k) of Theorem 4.

Case V: $\mathbf{B_2 \neq 0}$, $\mathbf{C_1C_3 < 0}$. The expression (6) for the system in the local chart U_1 is

$$\begin{aligned} u' &= (1+u^2)v^2, \\ v' &= -C_1 - C_3u^2 - B_2uv^2 - A_1v^2 + uv^3. \end{aligned} \tag{17}$$

So there are two singular points at infinity, $p_1 = (\sqrt{-C_1/C_3}, 0)$ and $p_2 = (-\sqrt{-C_1/C_3}, 0)$. Similarly in the chart U_2 the origin O_{U_2} is a singularity, because this system writes

$$\begin{aligned} u' &= -(1+u^2)v^2, \\ v' &= -C_3u - C_1u^3 - B_2uv - A_1uv^2 - uv^3. \end{aligned} \tag{18}$$

The linear parts of system (17) at p_1 and p_2, and of system (18) at O_{U_2} are respectively

$$\begin{pmatrix} 0 & 0 \\ -2C_3\sqrt{-C_1/C_3} & -B_2\sqrt{-C_1/C_3} \end{pmatrix},$$
$$\begin{pmatrix} 0 & 0 \\ 2C_3\sqrt{-C_1/C_3} & B_2\sqrt{-C_1/C_3} \end{pmatrix},$$
$$\begin{pmatrix} 0 & 0 \\ -C_3 & 0 \end{pmatrix}.$$

The singular points p_1 and p_2 are semi-hyperbolic singularities. By Theorem 2.19 of [11], p_1 and p_2 are saddle–nodes. We remark that in **Case IV**, which only differs from the present one by the vanishing of the coefficient B_2, the two singular points p_1 and p_2 in the chart U_1 are cusps. Both cusps and saddle–nodes are singular points of index 0. The cusps in the previous case bifurcate to saddle–nodes by changing B_2 from zero to non-zero values.

The local phase portraits at p_1 and p_2 depend on the values of the coefficients A_1, B_2, C_1 and C_3. The possible local phase portraits are shown in Figs. 25–29. These local phase portraits are obtained as in case I.1.1.

The point O_{U_2} in the chart U_2 is a nilpotent singular point. Applying Theorem 3.5 of [11] we see that it is a cusp, whose behavior depends on the sign of the coefficient C_3. Hence the local phase portrait at the origin for system (7) might be one of the two shown in Fig. 2.

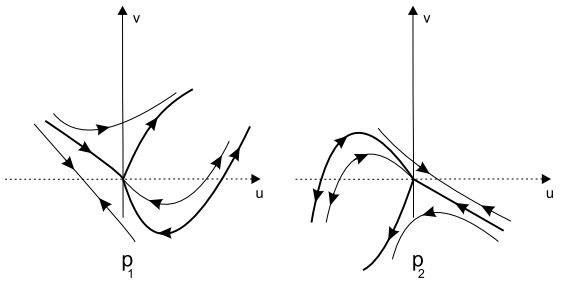

Fig. 26. Phase portrait of system (5) for $C_1 > 0,\ A_1, B_2, C_3 < 0$.

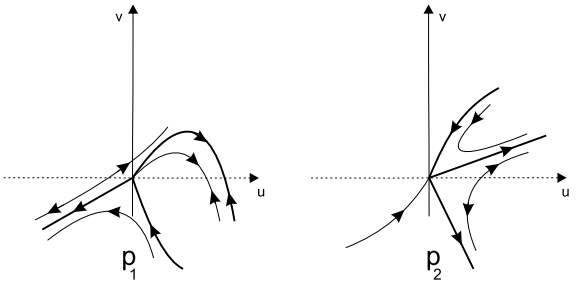

Fig. 27. Phase portrait of system (5) for $A_1, C_3 > 0,\ B_2, C_1 < 0$.

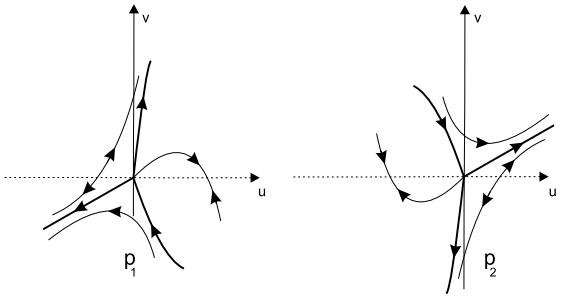

Fig. 28. Phase portrait of system (5) for $C_3 > 0,\ A_1, B_2, C_1 < 0$.

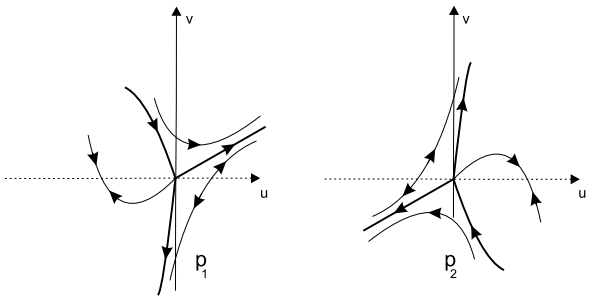

Fig. 29. Phase portrait of system (5) for $A_1 \in \mathbb{R},\ B_2, C_1 > 0,\ C_3 < 0$.

Using similar arguments as in the previous cases, we shall have three possible configurations for the global phase portraits, they are shown in Fig. 1(l), (m) and (n) of Theorem 4. We remark that all three configurations are possible, setting $B_2 = \varepsilon > 0$ in the examples presented in **Case IV**.

Acknowledgments

The first author is supported by a Ciência sem Fronteiras-CNPq grant number 201002/2012-4 and partially supported by a MINECO/FEDER grant MTM2008-03437 and MTM2013-40998-P, an AGAUR grant number 2014SGR-568, an ICREA Academia, the grants FP7-PEOPLE-2012-IRSES 318999 and 316338, grant UNAB13-4E-1604, and a CAPES grant 88881. 030454/2013-01 do Programa CSF-PVE.

References

[1] G.R. Fowles, G.L. Cassiday, Analytical Mechanics, Thomson Brooks/Cole, 2005.
[2] A.G. Choudhury, P. Guha, On commuting vector fields and Darboux functions for planar differential equations, Lobachevskii J. Math. 34 (2013) 212–226.
[3] A. Algaba, M. Reyes, Characterizing isochronous points and computing isochronous sections, J. Math. Anal. Appl. 355 (2009) 564–576.
[4] J. Chavarriga, M. Sabatini, A survey of isochronous centers, Qual. Theory Dyn. Syst. 1 (1999) 1–70.
[5] R. Conti, Uniformly isochronous centers of polynomial systems in $\mathbb{R}^2$, Lect. Notes Pure Appl. Math. 152 (1994) 21–31.
[6] M. Han, V.G. Romanovski, Isochronicity and normal forms of polynomial systems of ODEs, J. Symbolic. Comput. 47 (2012) 1163–1174.
[7] A. Algaba, M. Reyes, T. Ortega, A. Bravo, Campos cuárticos con velocidad angular constante, in: Actas: XVI CEDYA Congreso de Ecuaciones Diferenciales y Aplicaciones, VI CMA Congreso de Matemática Aplicada. Vol. 2, Las Palmas de Gran Canaria, 1999, pp. 1341–1348.
[8] J. Chavarriga, I.A. García, J. Giné, On the integrability of differential equations defined by the sum of homogeneous vector fields with degenerate infinity, Internat. J. Bifur. Chaos Appl. Sci. Engrg. 11 (2001) 711–722.
[9] H. Poincaré, Mémoire sur les courbes définies par les équations différentielles, J. Math. 37 (1881) 375–422;
Oeuvres de Henri Poincaré, Vol. I, Gauthier-Villars, Paris, 1951, pp. 3–84.
[10] M.A. Lyapunov, Probléme Général de la Stabilité du Mouvement, in: Ann. of Math. Stud., vol. 17, Princeton University Press, 1947.
[11] F. Dumortier, J. Llibre, J.C. Artés, Qualitative Theory of Planar Differential Systems, in: Universitext, Springer-Verlag, 2006.
[12] E.A. González, Generic properties of polynomial vector fields at infinity, Trans. Amer. Math. Soc. 143 (1969) 201–222.
[13] D. Neumann, Classification of continuous flows on 2-manifolds, Proc. Amer. Math. Soc. 48 (1975) 73–82.
[14] J. Itikawa, J. Llibre, Limit cycles for continuous and discontinuous perturbations of uniform isochronous cubic centers, J. Comput. Appl. Math. 277 (2014) 171–191.